Conformational Features of Poly(methylphenylsilylene)

P. R. Sundararajan

Xerox Research Centre of Canada, 2660 Speakman Drive, Mississauga, Ontario, Canada L5K 2L1. *Received August 24, 1987*

ABSTRACT: The conformational energies and helix parameters were calculated for the various states of the poly(methylphenylsilylene) (PMPS) chain, in terms of the rotations around two successive skeletal bonds. The calculations were performed for the three different relative dispositions of the phenyls attached to three successive silicon atoms. The minima are invariably shifted from perfectly staggered positions. The significant shift of the minimum in the tt state results in a nonrectilinear shape for the chain segment. The possible correlations between the a priori probability of bond conformations and the spectroscopic observation on the variation of UV absorption maximum with degree of polymerization for the oligomers and the change in the peak characteristics upon reducing the temperature to 77 K are explored. The conformations as well as the characteristic ratio are interpreted in terms of the helix parameters. The large experimental value of the characteristic ratio is reproduced by a chain that is stereoirregular.

Introduction

Polysilylenes have attracted considerable interest in recent years due to their potential for multifaceted applications such as precursors to β-SiC fibers, impregnating agents for ceramics, photoresists, photoinitiators for vinyl polymerization, semiconductors upon doping, etc. Due to the strong optical absorption in the near-UV region, a number of studies have been reported on the spectroscopic of poly(organosilylene).[1-6] The absorption is found to be conformation dependent. For example, the thermochromic behavior that has been observed in the case of poly(di-*n*-hexylsilylene) is accompanied by structural changes, as observed by X-ray diffraction.[7] Because of the strong influence of the conformation on the properties, an understanding of the preferred conformations becomes important.

The conformational analyses of polysilane,[8-10] poly(dimethylsilylene),[8,10] and poly(di-*n*-hexylsilylene)[11] have been reported in the literature. These are symmetrically substituted chains. The asymmetrically substituted chains such as poly(methylphenylsilylene) (PMPS) have also been studied spectroscopically[5] as well as for their electronic transport properties.[12] The PMPS chain has a phenyl substituent that is planar and a methyl side group that can be treated as a hard sphere. In this respect, it resembles the vinyl chain poly(α-methylstyrene). It has been shown[12] that the hole transport in polysilylenes, including PMPS, involves states derived from the backbone. The transport in PMPS is strikingly similar to that in poly(*N*-vinylcarbazole) (PVK). However, in PVK the transport involves not the carbon backbone but direct hopping among the pendant carbazole side groups. The conformational features of poly(α-methylstyrene) and PVK have been described before.[13,14] The relative energies of the various skeletal conformations were analyzed in terms of the meso and racemic configurations of the diads. In this paper, the conformational analysis of the PMPS chain is reported, in terms of the stereochemical configuration of the successive skeletal bonds.

Description of the Configuration

A schematic of the PMPS chain is shown in Figure 1. In the calculations on the analogous asymmetric vinyl chains, the chain is treated as a sequence of meso and racemic diads.[13-15] The first- and second-order interactions are considered in estimating the relative energies of the various isomeric states of the diads. The former depends on the rotation about one skeletal bond, whereas the second-order interactions involve rotations about two successive skeletal bonds, i.e., the two C–C_α bonds spanning the methylene group and those spanning the C_α atom.[15]

The conformations of the PMPS chain can be treated in a similar fashion. However, the presence of nonhydrogen substituents on successive Si atoms introduces additional features. Consider the successive Si atoms, as shown in Figure 1. With respect to the plane of the skeletal bonds in the planar all-trans conformation, the phenyl groups on $(Si)_{i-1}$, $(Si)_i$, and $(Si)_{i+1}$ can be all up, all down, or alternate. A total of eight configurations are possible as follows: (1) (up, up, up); (2) (down, down, down); (3) (up, down, up); (4) (down, up, down); (5) (up, up, down); (6) (down, down, up); (7) (down, up, up); (8) (up, down, down). If the chain ends are indistinguishable, degeneracy reduces the number of distinct configurations to three. Thus, (1) and (2) are equivalent; so are (3) and (4) and (5-8). Hence, in treating the chain in terms of the configuration of the phenyl group on three successive Si atoms, the three configurations in which the phenyl groups on $(Si)_{i-1}$, $(Si)_i$, and $(Si)_{i+1}$ are (up, up, up), (up, down, up), and (up, up, down) are considered in the following calculations. Perpetuation of the (up, up, up) sequence corresponds to the syndiotactic polymer, while the (up, down, up) and (up, up, down) sequences lead to isotatic and heterotactic segments, respectively.

To define the stereochemical character of the diads in an asymmetric vinyl chain and to relate the corresponding coordinate system of one bond to the next, Flory et al.[15] considered the bonds rather than the C_α atoms as loci of chirality. The meso diad is then composed of a *dl* or *ld* bond pair. The successive bonds are mirror images of each other. A sequence of *dd ll dd* bonds comprises the syndiotactic chain. A similar relationship exists between the successive bonds in the PMPS chain.

A view of the projection down the bonds i and $i + 1$ in a PMPS chain is shown in Figure 1, for the (up, up, up), (up, down, up), and (up, up, down) configurations of the groups $(Ph)_{i-1}$, $(Ph)_i$, and $(Ph)_{i+1}$. When the phenyls $(Ph)_{i-1}$ and $(Ph)_{i+1}$ are both in the up configuration, a mirror relationship exists between the bonds i and $i + 1$, centered about $(Si)_i$. This applies to the (up, up, up) and (up, down, up) configurations. However, for the (up, up, down) configuration, this mirror relationship is lost. This feature is used in a fashion analogous to the treatment of vinyl chains,[15] in defining the right- and left-handed coordinate systems for constructing the transformation matrices.

Energy Calculations

The Lennard-Jones 6-12 potential function was used to calculate the nonbonded interaction energies. The pa-

0024-9297/88/2221-1256$01.50/0

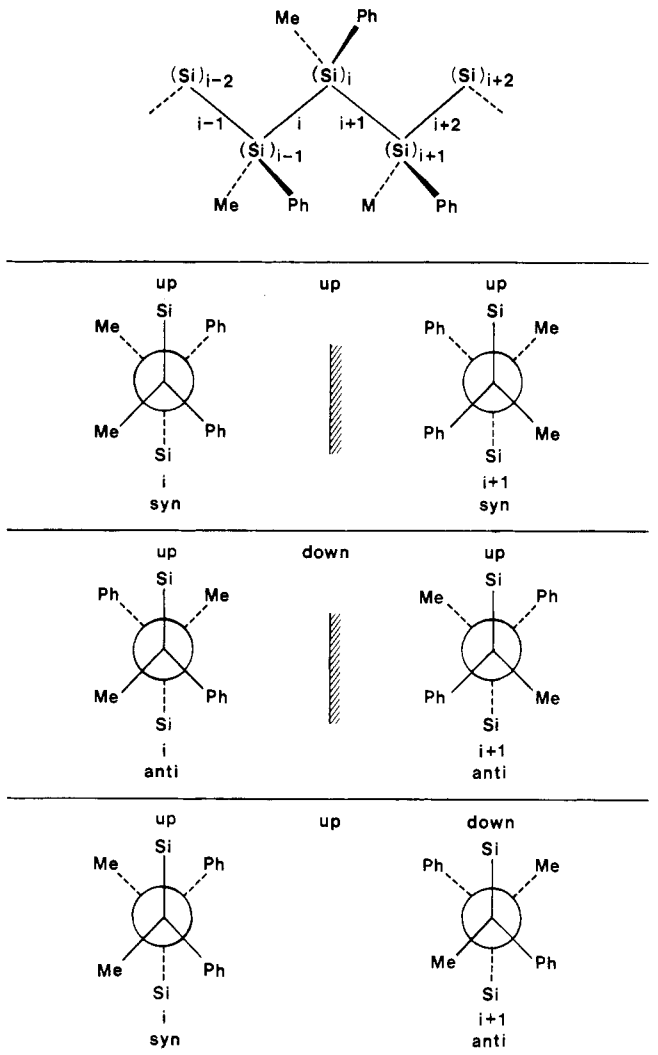

Figure 1. Schematic of a segment of the PMPS chain. The relationship between successive bonds for the various configurations of the phenyl group is shown.

Table I
Parameters for Nonbonded Energy Calculations

atom	polarizability, Å^3	effective no. of electrons	van der Waals radius, Å
Si	2.8	13	2.05
C_{ar}	1.23	5	1.85
(CH_3)	1.77	7	1.9
H	0.42	0.9	1.2

rameters employed are similar to those used previously[10,13] and are listed in Table I. A torsional barrier of 1.2 kcal mol^{-1} was included for the rotations of the Si–Si bonds. The bond lengths and bond angles are given in Table II. A value of 116° was used for the bond angle Si–Si–Si. Although a larger value of 122–124° was required for the analogous vinyl chain poly(α-methylstyrene),[13] the C–C bond length is considerably shorter than the Si–Si bond length.

The planar all-trans conformation defines the rotational state $\Phi_i = \Phi_{i+1} = 0$. The angles Φ_i and Φ_{i+1} were varied at intervals of 10° each. For each of these rotations, the positions of $(Ph)_{i-1}$, $(Ph)_i$, and $(Ph)_{i+1}$ were varied from −20° to +20° about the corresponding C–Si bond, and the positions that led to the least energy were included in calculating the overall nonbonded interaction energy for that Φ_i,Φ_{i+1} state. The methyl groups were treated as hard spheres. For each of the rotational states of the skeletal bonds, all the nonbonded interactions between groups appended to $(Si)_{i-1}$, $(Si)_i$, and $(Si)_{i+1}$ were summed up.

Table II
Geometric Parameters

atoms in bond	bond length, Å	atoms in bond	bond angle, deg
Si–Si	2.34	Si–Si–Si	116
Si–C	1.87	Si–Si–C	109
Si–C_{ar}	1.87	Si–Si–C_{ar}	109
C_{ar}–C_{ar}	1.39	C–Si–C_{ar}	104.2
C_{ar}–H	1.10	C_{ar}–C_{ar}–C_{ar}	120

Thus, the energies include both the first- and second-order interactions. Substituents on the atoms $(Si)_{i-2}$ and $(Si)_{i+2}$ may give rise to repulsive interactions if one of the bonds is in the g or $\bar{g}$ conformation. In this case, interactions beyond the two bond rotations may have to be included. Rotations of pairs of bonds in terms of Φ_{i-1}, Φ_i, Φ_{i+1}, and Φ_{i+2} should be considered collectively, in the manner described before.[15] However, this is not attempted here. Due to the significant shift of the minima from perfect staggering, select calculations at the minima, including the $(Ph)_{i-2}$ and $(Me)_{i-2}$ showed that no adverse interactions occur if one of the bonds is in the g or $\bar{g}$ conformation. For the $\bar{g}\bar{g}$ state, the statistical weight based on the two bond rotations is low. The conformational partition function Z, the average energy $\langle E \rangle$, and the average locations of the rotational states $\langle \Phi_i,\Phi_{i+1} \rangle$ were calculated in the usual manner[13] for each of the rotational isomeric states.

Helix Parameters

If a given set of values of the rotations Φ_i and Φ_{i+1} perpetuate over a few successive bonds in the chain, the segment would adopt a helical shape. In discussion of the perpetuation of the possible conformations, it is useful to consider the type of helical shape of the segment. Irrespective of the length of the sequence of the skeletal bonds in a given conformation, the shape of the segment as discerned from the helix parameters aids in understanding the overall features of the chain.

The helix parameters n, the number of units per turn of the helix, and h, the advance per unit along the helix axis (pitch = nh), were calculated as described before.[16] Since the energy calculations were performed with pairs of skeletal bonds, the helix parameters were calculated on the same basis, i.e., the part of the chain from $(Si)_{i-1}$ to $(Si)_{i+1}$ is taken to be the repeat unit. This comprises two skeletal bonds. Hence, for a given n, the number of skeletal bonds per turn of the helix is $2n$.

Results and Discussion

Energy Maps. The energy maps in terms of Φ_i and Φ_{i+1} are shown in Figures 2–4, for the (up, up, up), (up, down, up), and (up, up, down) configurations of the phenyls on three successive Si atoms. The contours are drawn relative to the minimum corresponding to the tt state in Figure 2. The values of Z, $\langle E \rangle$, and $\langle \Phi_i,\Phi_{i+1} \rangle$ are given in Table III. The iso contours of the helix parameters n and h are shown in Figure 5. The negative values of h correspond to left-handed helices in this figure. For $(\Phi_i,\Phi_{i+1}) = (0,0)$, the chain is rectilinear, and hence the value of $h = 0$ does not apply to this state.

In the energy maps shown in Figures 2–4, the minima are shifted from perfect staggering. Significant displacement of minima from perfect staggering has been calculated for the analogous vinyl chain, poly(α-methylstyrene).[13] Similar is the case for some of the states of poly(dimethylsilylene).[10] In Figure 2 for the (up, up, up) configuration, the minimum in the tt region is split and occurs at $(\Phi_i,\Phi_{i+1}) = (0,-30°)$ and $(-30°,0)$. The barrier between them is less than 0.5 kcal mol^{-1}. While the perpetuation with $(\Phi_i,\Phi_{i+1}) = (0,0)$ would generate a rectilinear

Table III
Average Parameters Derived from Energy Calculations

configuration	state	Z	$\langle E \rangle$, kcal mol^{-1}	Z/Z_0	ζ_0	$\langle \Phi_i, \Phi_{i+1} \rangle$, deg
(up,up,up)	tt	19.52	0.46	1	1	-8.6,-8.7
	tḡ	0.33	2.91	0.017	1.06	-11.3,-113.2
(up,down,up)	tt	2.81	1.51	0.144	0.84	-8.1,-8.3
	tḡ	0.86	2.23	0.044	0.86	-16.4,-101.1
	ḡḡ	1.48	1.93	0.076	0.91	-124,-124
(up,up,down)	tt	1.44	2.01	0.073	1	-35.6,-20.9
	tḡ	8.73	0.82	0.45	0.83	1.4,-107
	ḡt	0.86	2.03	0.044	0.62	-106.3,-1.5
	ḡḡ	0.10	3.24	0.005	1.25	121.7,-119.8

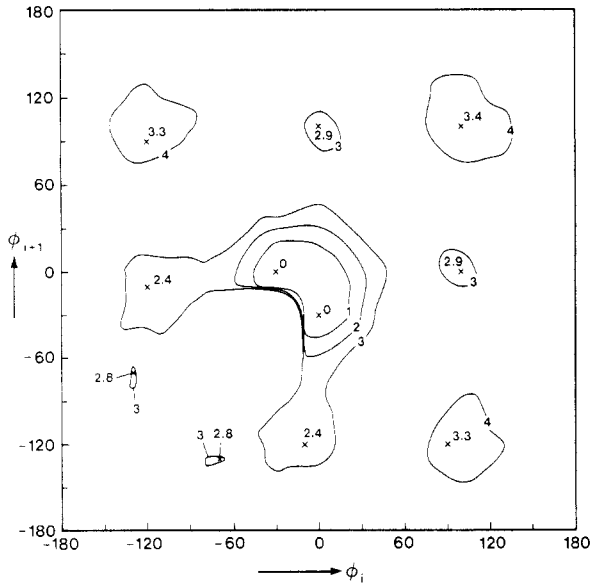

Figure 2. Isoenergy contours are shown in terms of Φ_i and Φ_{i+1} for the (up, up, up) configuration of the phenyl groups on $(Si)_{i-1}$, $(Si)_i$, and $(Si)_{i+1}$. Contours are drawn relative to the minimum in the tt state.

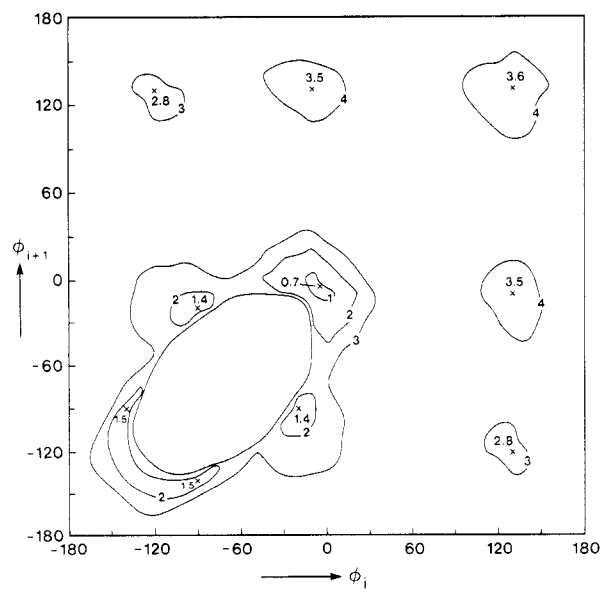

Figure 3. Same as Figure 2, but for the (up, down, up) configuration of the phenyl groups. Contours are drawn relative to the minimum in the tt state in Figure 2.

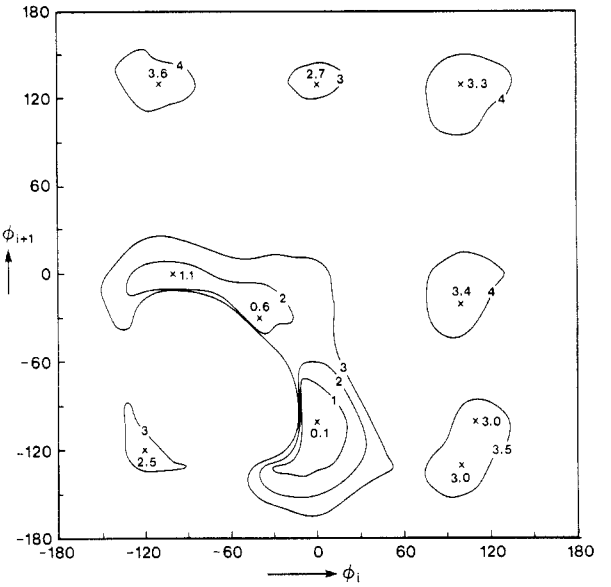

Figure 4. Same as Figure 3, but for the (up, up, down) configuration of the phenyl groups.

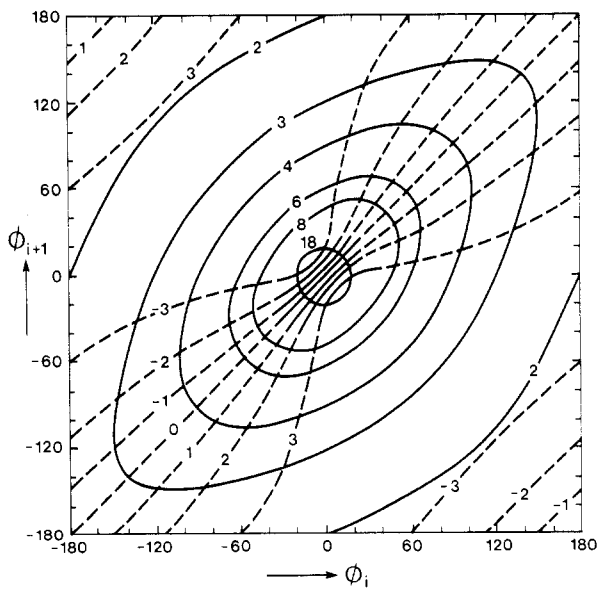

Figure 5. Isocontours of helix parameters n (solid curves) and h (broken curves) for the PMPS chain. Negative values of h denote left-handed helices. The sign of the angle Φ_{i+1} on the ordinate should be reversed when applying this map to the (up, up, down) configuration.

chain segment, the shift of the rotational states to (0,-30°) or (-30°,0) would lead to a slowly winding helical segment. From comparison of Figures 2 and 5, the conformations (0,-30°) and (-30°,0) correspond to left- and right-handed helical segments, respectively, with n = 12 and h = 3.37 Å (i.e., 24 bonds in a pitch of 40.44 Å). The tḡ (or ḡt) conformation is 2.4 kcal mol^{-1} higher in energy than the tt state. In this case, the minima are shifted to (-10,-120°) or (-120,-10°). A significant shift of the ḡḡ state to (-50°,-130°) and (-130°,-50°) is also noted. The g state is of high energy. Thus, for the (up, up, up) configuration, a predominant preference for the tt state is indicated.

For the (up, up, up) and (up, down, up) configurations, the second-order interactions are the same. The differences between the energy maps in Figures 2 and 3 can be attributed to the difference in the first-order interactions. The energy contours in Figure 3 for the (up, down, up) configuration show that the minimum for the tt state is shifted marginally, to $(\Phi_i,\Phi_{i+1}) = (-5°,-5°)$. The large shift in the tt minimum in Figure 2 compared to that in Figure 3 can be rationalized on the basis of the first-order interactions. Figure 1 shows that if the phenyls attached to $(Si)_{i-1}$ and $(Si)_i$ are both in the up configuration, the phenyls are syn to each other and so are the methyls with respect to each other. However, if $(Ph)_{i-1}$ and $(Ph)_i$ are in the up, down configuration, the two phenyls are trans to each other and so are the methyl groups. The minimum for the $t\bar{g}$ conformation in Figure 3 is shifted significantly from perfect staggering to (-20°,-90°). The $\bar{g}\bar{g}$ state shows split minima at (-90°,-140°) and (-140°,-90°). Both $t\bar{g}$ and $\bar{g}\bar{g}$ conformations are only 700 cal mol^{-1} higher in energy than the tt state in this case. The g state is of high energy.

Comparison of Figures 3 and 5 shows that corresponding to the tt minimum at $(\Phi_i,\Phi_{i+1}) = (-5°,-5°)$, the helix parameters are $n = 67.9$ and $h = 0$. Thus, the perpetuation of a segment in this conformation would cause a looping effect. For the minimum in the $t\bar{g}$ state with $(\Phi_i,\Phi_{i+1}) = (-20°,-90°)$, the helix parameters are $n = 4.35$ and $h = 2.92$ Å (i.e., 8.7 bonds in a pitch of 12.7 Å). The $\bar{g}\bar{g}$ state with $(\Phi_i,\Phi_{i+1}) = (-90°,-140°)$ corresponds to a helix with $n = 3.11$ and $h = 1.68$ Å (6.22 bonds in a pitch of 5.24 Å). Thus, a sequence of the chain in the (up, down, up) configuration would lead to compact helical and looping segments.

The energy contours in Figure 4 for the (up, up, down) configuration differ appreciably from those in Figures 2 and 3. This configuration resembles the racemic diad of the analogous vinyl chain. The g states are of high energy in this case as well. The tt state is shifted significantly to (-40°,-30°). The first-order interactions arising from the Φ_i rotation differ from those due to the Φ_{i+1} rotation. Hence, the map lacks the symmetry that is seen in Figures 2 and 3. The $t\bar{g}$ minimum is shifted to $(\Phi_i,\Phi_{i+1}) = (0,-100°)$ and is lower in energy than the tt minimum, by 0.5 kcal mol^{-1}. The minimum for the $\bar{g}t$ state, which occurs at (-100°,0), is higher in energy by 0.5 kcal mol^{-1} than the minimum for the tt state. The barrier between the tt and $\bar{g}t$ states is 0.5 kcal mol^{-1}. The $\bar{g}\bar{g}$ state is higher in energy than the tt state by 1.9 kcal mol^{-1}.

Figure 5 shows that the helix parameters for $(\Phi_i,\Phi_{i+1}) = (-40°,-30°)$ are $n = 6.07$ and $h = -3.9$ Å (i.e., 12.14 bonds in a left-handed helix with a pitch of 23.67 Å). The minimum in the $t\bar{g}$ state, with $(\Phi_i,\Phi_{i+1}) = (0,-100°)$ would lead to a helix with $n = 3.6$ and $h = -3.37$ Å, whereas the $\bar{g}t$ minimum would result in the corresponding left-handed helix.

Thus, the calculations on PMPS show that one of the bonds being in the g state leads to high energy. This is due to the second-order interactions. The preference for the $t\bar{g}$ and $\bar{g}\bar{g}$ states relative to the tt state depends on the configuration of the phenyl groups on successive Si atoms. Slowly winding or compact helical types of segments occur depending on the local configuration.

It has been observed that the hole transport in PMPS is associated with the chain backbone but remains relatively localized.[12] The transport is also similar to that in PVK, which involves the pendant carbozole groups. In PVK, the near tt state of the meso diad allows the adjacent carbozole groups to be within the proximity required for the hole hopping. The occurrence of the tg state or the racemic diad interrupts continuity along the entire length of the chain. In the case of PMPS, the predominant preference for the tt state for the (up, up, up) configuration assures continuity in the transport along the backbone if this steric configuration perpetuates along the entire chain. However, the occurrence of the $t\bar{g}$ or an occasional $\bar{g}\bar{g}$ conformation of the (up, down, up) or (up, up, down) configurations can facilitate hopping between nonconsecutive Si atoms. For example, for the (up, down, up) configuration in the $t\bar{g}$ state, with $(\Phi_i,\Phi_{i+1}) = (-20°,-90°)$, the distances $(Si)_{i-2}$–$(Si)_{i+1}$ and $(Si)_{i-1}$–$(Si)_{i+2}$ are 6.04 and 5.3 Å, respectively. Thus, hopping between nonconsecutive Si atoms along the chain may account for the localized behavior of hole transport, and stereoirregularity would then be a contributing factor.

Table III shows the statistical weights for the various states, relative to a weight of 1 for the tt state of the (up, up, up) configuration. The preexponential factors[13] ζ_0 for the Boltzmann expression for the statistical weights are also given in this table. Description of the statistical weights in terms of symbols is not attempted here, due to their large number. When the interaction between the various atoms or groups are considered, there are six nonequivalent statistical weights for second-order interactions between Ph, Me, and Si and another six for the first-order interactions. The task is simplified in the case of analogous vinyl chains,[15] due to treating CH_2 and CH_3 groups as equivalent and assigning a weight of 1 for interactions involving hydrogen atoms. A further complication in this case is that the Ph···Ph interaction in the tt state (in which the planes of the phenyl groups are nearly parallel) is not the same as in the $\bar{g}\bar{g}$ state. Due to these constraints, the statistical weight matrices were constructed by using the data given in Table III, without resort to the symbolic representation. The statistical weight matrices for the bond pair i and $i + 1$ in the three configurations are

$$\mathbf{U}_{(up,up,up)} = \begin{bmatrix} 1 & 0.017 \\ 0.017 & 0 \end{bmatrix} \quad (1)$$

$$\mathbf{U}_{(up,down,up)} = \begin{bmatrix} 0.144 & 0.044 \\ 0.044 & 0.076 \end{bmatrix} \quad (2)$$

$$\mathbf{U}_{(up,up,down)} = \begin{bmatrix} 0.073 & 0.447 \\ 0.044 & 0.005 \end{bmatrix} \quad (3)$$

These matrices are based on the t and $\bar{g}$ states of the bonds, the g state having been excluded.

A Priori Bond Probability

Spectroscopically it is observed that in the case of oligomers of PMPS, the UV absorption maximum red shifts up to a degree of polymerization (DP) of 40 and reaches an asymptotic value thereafter.[1] In addition, the absorption spectrum at room temperature shows a structureless band, whereas a significant change in the spectrum occurs at 77 K, with a large increase in the intensity of the band.[5] These observations are attributed to conformational effects.[1,5] In particular, the transformation of the band width when the temperature is reduced to 77 K has been interpreted as due to a freezing in of the chain in the tt state.

The possible relationship between the above conformational effects and the a priori probability that a bond i in the chain occurs in a state η is explored here. Jernigan and Flory[17] developed methods to calculate such probabilities. The first-order a priori probability that a bond i occurs in a state η is given by

$$p_{\eta,i} = Z^{-1}J^*[\prod_{h=2}^{i-1}\mathbf{U}_h]\mathbf{U}'_{\eta,i}[\prod_{j=i+1}^{n-1}\mathbf{U}_j]J \quad (4)$$

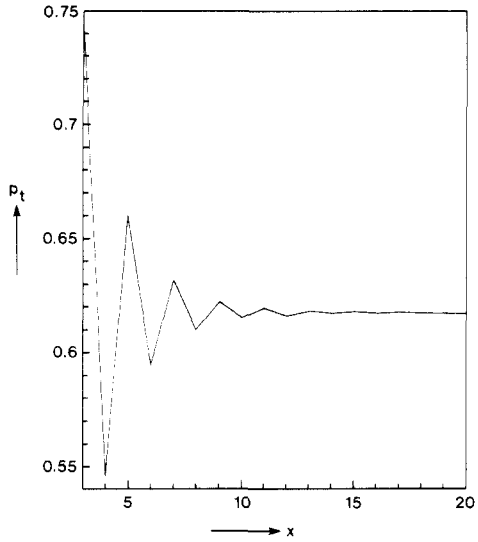

Figure 6. First-order a priori bond probability p_t is shown as a function of the location of the bond in the chain, with the (up, up, down) configuration.

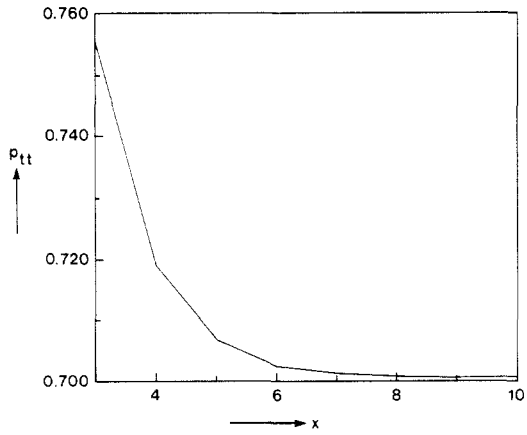

Figure 7. Second-order a priori bond probability p_{tt} is shown as a function of the location of the bonds $i-1$ and i in the chain, for the (up, down, up) configuration.

where $\mathbf{U}'_{\eta;i}$ is the matrix obtained from $\mathbf{U}_i$, by replacing all the elements except those of column η by zeros. Z is the partition function given by

$$Z = J^*[\prod_{j=2}^{n-1}\mathbf{U}_j]J \tag{5}$$

$$J^* = [1\ 0\ \ldots\ 0] \qquad J = \text{col}\ [1\ 1\ 1\ \ldots\ 1] \tag{6}$$

The second-order a priori probability that the bonds $i-1$ and i occur simultaneously in states ζ and η is given by

$$p_{\zeta\eta;i} = Z^{-1}J^*[\prod_{h=2}^{i=1}\mathbf{U}_h]\mathbf{U}'_{\zeta\eta;i}[\prod_{j=i+1}^{n=1}\mathbf{U}_j]J \tag{7}$$

where $\mathbf{U}'_{\zeta\eta;i}$ is the matrix obtained by replacing all the elements except that of $\zeta\eta$ with zeros.

The location of the bonds $i-1$ and i was varied along the chain, from $x = 3$ to 20, in a chain containing 50 units (100 bonds). Figure 6 shows the variation of p_t for bond i in units $x = 3$–20, in a chain with the (up, up, down) configuration. A temperature of 300 K was used. It is seen that p_t oscillates significantly up to $x = 10$ and minor oscillation persists up to $x = 20$ (40 bonds). Thus, the chain-end effect propagates for a number of units. In contrast, for the polyethylene chain,[17] the p_t reaches the asymptotic value with five bonds.

Figures 7 and 8 illustrate the variation of p_{tt} and $p_{\bar{g}t}$ for the (up, down, up) and (up, up, down) configurations, respectively. For the former, the p_{tt} decreases with x and

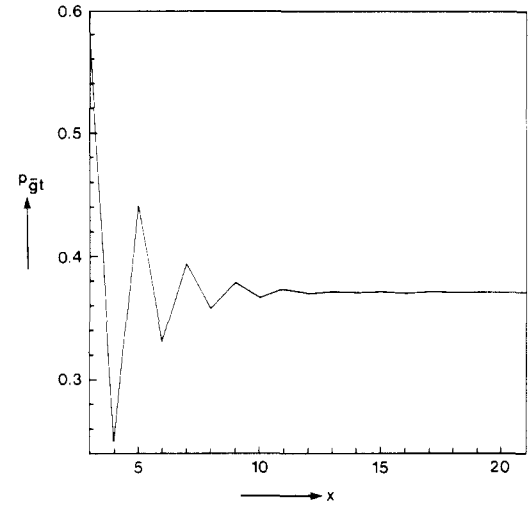

Figure 8. Second-order a priori bond probability $p_{\bar{g}t}$ is shown as a function of the location of the bonds $i-1$ and i in the chain, for the (up, up, down) configuration.

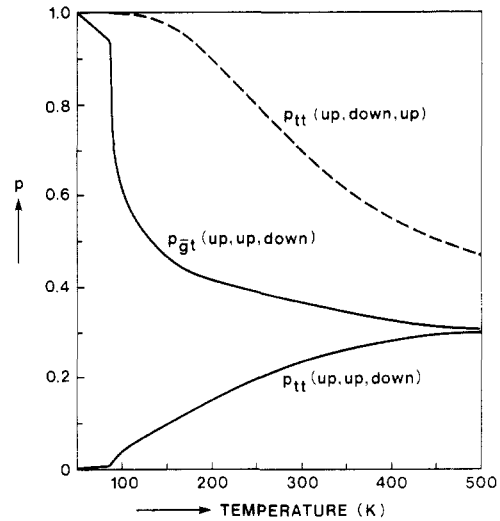

Figure 9. Variation of the second-order a priori bond probabilities with temperature.

reaches the asymptotic value for $x \geq 10$ (20 bonds). On the other hand, the $p_{\bar{g}t}$, in Figure 8 shows oscillation with x and reaches a constant value for $x \geq 20$ (40 bonds). In the case of the (up, up, up) configuration, for which the tt state is highly preferred, the bond probabilities, p_t and p_{tt} are close to 1 and do not show variations with x.

Figure 9 shows the variation of the asymptotic values of the second-order bond probabilities as a function of temperature. At 50 K, p_{tt} for the (up, up, down) configuration is zero. Between 70 and 100 K, the value begins to increase. The $p_{\bar{g}t}$ for this configuration is 1 at 50 K. It shows a significant decrease between 70 and 100 K. At about 500 K, the p_{tt} and $p_{\bar{g}t}$ become equal. For the (up, down, up) configuration, p_{tt} is 1 at 50 K. It gradually decreases with increase in temperature.

Thus, the present calculations show that for the (up, up, up) configuration, the bond probabilities p_t and p_{tt} are close to 1 at 300 K and do not show a chain-end effect. However, with the (up, down, up) and (up, up, down) configurations, the first- and second-order bond probabilities show variations up to 40 bonds. Hence, it would seem that the occurrence of the (up, down, up) and (up, up, down) configurations and the oscillation of the bond probabilities contribute to the red shift of the absorption maximum with DP for the oligomers.[1] The sharpening of the absorption peak[5] upon reducing the temperature to 77

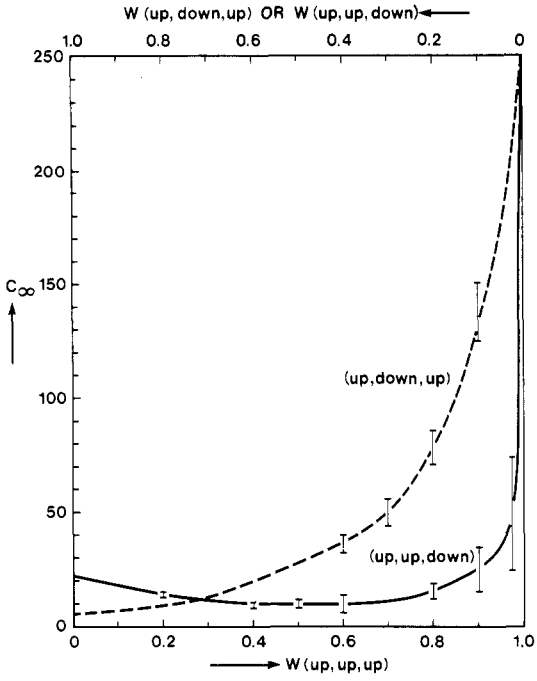

Figure 10. Characteristic ratio C_∞ is shown as a function of the fraction of (up, down, up) or (up, up, down) and (up, up, up) configurations.

K may be attributed to the increase in p_{tt} of the segments in the (up, down, up) configuration. Hence, stereoirregularity might be the contributing factor for the above spectroscopic observations. Thus, there seems to be a correlation between the calculated bond probabilities and the spectroscopic observations. In such a case, the curves in Figure 9 would suggest a conformational transition above 500 K, where the p_{tt} and $(p_{\bar{g}t} + p_{t\bar{g}} + p_{\bar{g}\bar{g}})$ for the (up, down, up) configuration become equal. Whether such a good correlation between the bond conformational probabilities and the above spectroscopic data is fortuitous can be verified by calculations on other chains that show similar behavior.

Characteristic Ratios

Characteristic ratios, C_x, were calculated by following the methods described previously.[15] The transformations for the (up, up, up) and (up, down, up) configurations were the same as for the treatment of a meso diad of an asymmetric vinyl chain, and those for the (up, up, down) configuration corresponded to that of the racemic diad. In some of the conformations, e.g., the tt state for the (up, up, up) configuration, the (Φ_i,Φ_{i+1}) at which the actual minima occur differ significantly from the values of $\langle\Phi_i,\Phi_{i+1}\rangle$. With $\langle\Phi_i,\Phi_{i+1}\rangle$ = (-8.6°,-8.7°), a near chain closure is encountered, whereas with (Φ_i,Φ_{i+1}) = (0,-30°) or (-30°,0), where the minima occur, the helix parameters are n = 12 and h = ±3.37 Å (i.e., 24 bonds in a pitch of 40.44 Å). Such differences in the shape of the segments would, of course, influence the calculated values of C_∞. This has been demonstrated in the calculations on poly(methyl methacrylate).[18] Although calculations were performed with both sets of rotational angles, only the results obtained by using the values of the rotation angles Φ_i,Φ_{i+1} corresponding to the actual location of the minima are described here. Where two minima occur, e.g., in the tt state of the (up, up, up) configuration, these are symmetrically placed. The helix parameters are the same, except for the sense of the helix. Hence, these were not treated as multiple states.

Figure 10 shows the variation of C_∞ for different fractions of (up, down, up) or (up, up, down) and (up, up, up) configurations. A value of 250 is obtained for C_∞ for a chain with 100% (up, up, up) configuration. The value of C_∞ decreases rapidly with about a 20% fraction of (up, down, up) or (up, up, down) configurations. Thus in the case of the (up, up, up) configuration, the perpetuation of near-trans helical conformation leads to a high value of C_∞. Cotts et al.[19] recently reported the dilute solution properties of several poly(organosilanes). For PMPS, they obtained a value of C_∞ = 64 ± 20. Figure 10 shows that such a large value is accounted for by a stereoirregular chain.

Registry No. PMPS (SRU), 76188-55-1.

References and Notes

(1) Trefonas, P.; West, R.; Miller, R. D.; Hofer, D. *J. Polym. Sci., Polym. Lett. Ed.* **1983**, *21*, 823.
(2) Harrah, L. A.; Zeigler, J. M. *J. Polym. Sci., Polym. Lett. Ed.* **1985**, *23*, 209.
(3) Miller, R. D.; Hofer, D.; Rabolt, J.; Fickes, G. N. *J. Am. Chem. Soc.* **1985**, *107*, 2172.
(4) Trefonas, P.; Damewood, J. R.; West, R.; Miller, R. D. *Organometallics* **1985**, *4*, 1318.
(5) Johnson, G. E.; McGrane, K. M. *ACS Symp. Ser.*, in press.
(6) Harrah, L. A.; Zeigler, J. M. *Macromolecules* **1987**, *20*, 601.
(7) Rabolt, J. F.; Hofer, D.; Miller, R. D.; Fickes, G. N. *Macromolecules* **1986**, *19*, 611.
(8) Damewood, J. R.; West, R. *Macromolecules* **1985**, *18*, 159.
(9) Bigelow, R. W.; McGrane, K. M. *J. Polym. Sci., Part B: Polym. Phys.* **1986**, *24*, 1233.
(10) Welsh, W. J.; DeBolt, L.; Mark, J. E. *Macromolecules* **1986**, *19*, 2978.
(11) Farmer, B. L.; Rabolt, J. F.; Miller, R. D. *Macromolecules* **1987**, *20*, 1167. Damewood, J. R. *Macromolecules* **1985**, *18*, 1793.
(12) Abkowitz, M.; Knier, F. E.; Yuh, H.-J.; Weagley, R. J.; Stolka, M. *Solid State Commun.* **1987**, *62*, 547.
(13) Sundararajan, P. R. *Macromolecules* **1977**, *10*, 623.
(14) Sundararajan, P. R. *Macromolecules* **1980**, *13*, 512.
(15) Flory, P. J.; Sundararajan, P. R.; DeBolt, L. C. *J. Am. Chem. Soc.* **1974**, *96*, 5015.
(16) Sundararajan, P. R. *Macromolecules* **1987**, *20*, 1534.
(17) Jernigan, R. L.; Flory, P. J. *J. Chem. Phys.* **1969**, *50*, 4165.
(18) Sundararajan, P. R. *Macromolecules* **1986**, *19*, 415.
(19) Cotts, P. M.; Miller, R. D.; Trefonas, P. T.; West, R.; Fickes, G. N. *Macromolecules* **1987**, *20*, 1046.